J. Phys. Chem. B **2008,** *112,* 6629–6635 **6629**

Physicochemical Characterization and Tube-like Structure Formation of a Novel Amino Acid-Based Zwitterionic Amphiphile *N*-(2-Hydroxydodecyl)-L-valine in Water

Arjun Ghosh and Joykrishna Dey*

Department of Chemistry, Indian Institute of Technology, Kharagpur 721 302, India

Received: December 27, 2007; Revised Manuscript Received: March 7, 2008

Surface activity and aggregation behavior of an amino acid-based zwitterionic amphiphile *N*-(2-hydroxydodecyl)-L-valine were studied in aqueous solutions (pH 13). The self-assembly formation was investigated by use of a number of techniques including surface tension, conductivity, viscosity, fluorescence spectroscopy, dynamic light scattering, and transmission electron microscopy. The amphiphile exhibits two breaks in the surface tension vs concentration plot indicating stepwise aggregate formation and thus results in two values of critical aggregation concentration. The amphiphile was found to be very surface active compared to fatty acid soaps. The average hydrodynamic diameter and size distribution of the aggregates were obtained from DLS measurements. Conductivity measurements suggested formation of vesicles or closed tubules. TEM pictures revealed the existence of spherical vesicles, separated tubules, and tubules with multiple Y-type junctions in going from dilute to moderately concentrated solution. However, in concentrated solution, the junctions break to form separate tubular structures which upon further increase of concentration are converted to rod-like micelles. The mechanism of branched tubule formation is discussed in light of the experimental observations.

Introduction

In recent years, molecular self-assembly has attracted considerable attention for its use in design and fabrication of nanostructures leading to the development of advanced materials.[1–5] Amphiphilic molecules self-assemble above a critical concentration, called critical aggregation concentration (CAC), to form aggregates of different shapes and sizes, such as micelles (spherical, disks, and rod-like), vesicles (spherical and tubules), and liquid crystals (hexagonal and lamellar) in aqueous solution.[6,7] Among these cylindrical nanotubes and helical ribbons are technologically most important.[8] Tubules and helical ribbons have been observed in a wide variety of amphiphiles including chiral surfactants.[9–11] Zhang and co-workers[12] have found branching tube-like structures in aqueous dispersions of peptide surfactants. On the other hand, Ghadiri and co-workers[13,14] demonstrated formation of self-assembling nanotubes of alternating D,L-α-peptides and cyclic *β*-peptides. These authors have suggested that monomeric peptide units first form segments of bilayer ring, which grows into single subunit rings and multirings. The tubular arrays then stack through backbone−backbone hydrogen-bonding interactions to form longer nanotubes. Tube-like structures were also observed with mixtures of cationic bolaamphiphile and anionic sodium dodecyl surfate (SDS).[15] In a recent report, Lu and co-workers[15c] have suggested salt-induced transformation of vesicles to tubules in a catanionic system consisting of a cationic bolaamphiphile and anionic SDS surfactant.

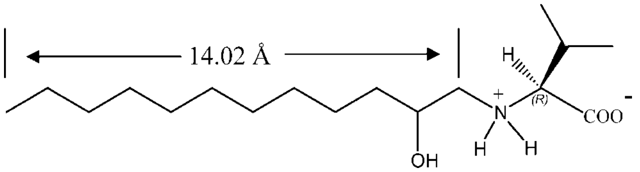

Figure 1. Molecular structure of *N*-(2-hydroxy-*n*-dodecyl)-L-valine (C_{12}HVal).

The present work is a part of our ongoing research interest in effects of molecular structure on the self-assembly properties and microstructure formation of chiral amphiphiles. For this study, we have chosen an *N*-alkylamino acid surfactant (AAS), *N*-(2-hydroxydodecyl)-L-valine, C_{12}HVal (see Figure 1). Hidaka et al. reported gelation of organic solvents by *N*-(2-hydroxydodecyl)-α-amino acids.[16] It has been demonstrated that these amphiphilic molecules exist in the fibrous helical aggregates in organic solvents. There are only a few reports on the aggregation behavior of AAS in water. Imae and co-workers[17] studied the aggregation behavior of *N*-(2-hydroxydodecyl)-L-aspartic acid (C_{12}HAsp) and found that at or above neutral pH, C_{12}HAsp does not generate any fibrous assemblies. This attracted our attention toward self-assembly properties of these amino acid-derived amphiphiles containing −OH group in the alkyl chain. Consequently, it seemed important to us to look at the type of self-assemblies that could be formed by C_{12}HVal in water. To characterize the microstructures of the self-assemblies, techniques such as surface tension, fluorescence, dynamic light scattering, and transmission electron microscopy were employed.

Results and Discussion

Critical Aggregation Concentration. It is widely recognized that surfactants form micelles, which are characterized by their critical micelle concentration (CMC). In the present work, we prefer the term "critical aggregation concentration" (CAC), as we show below that aggregates of other types can be formed by C_{12}HVal. The C_{12}HVal amphiphile being an inner salt is insoluble in water between pH 2 and 12. Consequently, all solutions were made in 0.1 M NaOH (pH 13) to ensure complete deionization of the ammonium group. It is assumed that at this pH, C_{12}HVal behaves as carboxylate, that is, as an anionic

---

* Author for correspondence. Phone: 91-3222-283308. Fax: 91-3222-255303. E-mail: joydey@chem.iitkgp.ernet.in

10.1021/jp712111d CCC: $40.75 © 2008 American Chemical Society
Published on Web 05/01/2008

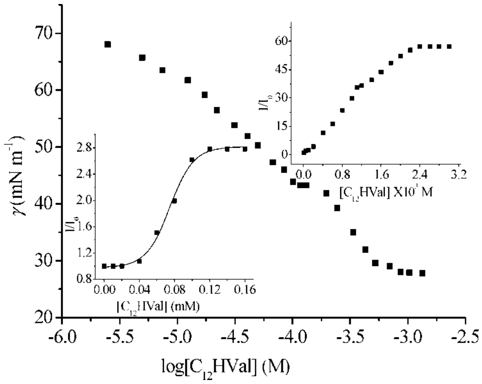

Figure 2. Plot of surface tension (γ) versus log [C_{12}HVal]. Inset: Plot of relative fluorescence intensity of NPN probe as a function of [C_{12}HVal].

TABLE 1: Physicochemical Parameters of C_{12}HVal in Aqueous Solution (pH 13) at 30 °C[a]

parameter	C_{12}HVal CAC$_1$	 CAC$_2$
CAC (mM)	0.08(0.07)	1.20(1.00)
γ_{CAC} (mN m^{-1})	43.44	28.13
pC_{20}	4.52	
CAC/C_{20}	2.53	38.0
$10^6\tilde{A}_{max}$ (mol m^{-2})	3.44	5.00
A_{min} (Å^2 molecule^{-1})	47.8	33.2
P	0.56	0.80

[a] Values within the parentheses were obtained from fluorescence probe studies.

surfactant. The CAC of the amphiphile was measured by use of surface tension and fluorescence probe methods. The surface tension value decreased nonlinearly with log [C_{12}HVal] and showed a characteristic break and remained constant thereafter (see Figure 2). A closer inspection of the plot shows two breaks, one at a concentration around 0.1 mM and another at around 1.0 mM. Our initial thought was that this might be due to some surface active impurity. However, the absence of any minimum around the second breakpoint confirmed the purity of the amphiphile. The purity of the compound was further confirmed by the ^{1}H and ^{13}C NMR spectra and elemental analysis data. Thus the concentrations corresponding to the first and second breakpoints can be taken as CAC$_1$ and CAC$_2$ values (see Table 1) of the amphiphile, respectively. The existence of two CAC values has also been reported for other surfactants[18–21] and mixed surfactant systems.[15a,b] This suggests that two types of aggregates of different morphologies are formed by C_{12}HVal in the concentration range studied.

To further substantiate the results of surface tension studies, we have performed fluorometric titration using *N*-phenyl-1-naphthylamine (NPN) as a probe molecule. The fluorescence spectrum of the NPN molecule is blue-shifted accompanied by a huge enhancement of fluorescence intensity in going from water to hydrocarbon solvent.[22] Therefore, it has been effectively used as a probe molecule for studying microenvironments of micelles.[23–28] The NPN probe being hydrophobic in nature normally gets solubilized in the hydrophobic core of micelles. In the presence of C_{12}HVal surfactant, the fluorescence emission spectrum (not shown) of NPN exhibits a blue shift of about 21 nm relative to that in water (pH 13) with a concomitant rise in intensity at a much lower concentration below CAC$_2$ indicating aggregate formation. The plot of relative fluorescence intensity (I/I_0) as a function of [C_{12}HVal] is shown in the inset (upper right) of Figure 2. Clearly, the plot shows two inflection points. To confirm the existence of the first inflection point in the plot we have performed the experiment separately in the dilute regime. The data are plotted in the inset (lower left) of Figure 2. The first and the second inflection points exactly correspond to the first and second breaks, respectively, in the surface tension plot. Also the CAC$_1$ and CAC$_2$ values (Table 1) obtained from the inflection points of the titration curve are close to the corresponding values obtained by the surface tension method. This confirms the stepwise aggregation of C_{12}HVal with two CAC values.

Interfacial Properties. The surface active parameters, such as CAC, surface tension corresponding to CAC (γ_{CAC}), and efficiency of adsorption (pC_{20} = negative logarithm of the surfactant concentration required to reduce the surface tension of water by 20 units), were determined from the surface tension plot in Figure 2. The values of the surface excess (Γ_{max}) and cross-sectional area per head group (A_{min}) at the interface were calculated by using the Gibbs adsorption equations:[6,29,30]

$$\Gamma_{max} = -\frac{1}{2.303nRT}\left(\frac{d\gamma}{d\log c}\right) \quad (1)$$

$$A_{min} = 1/N_A\Gamma_{max} \quad (2)$$

where dγ/d log c is the maximum slope; N_A is Avogadro's number; T = absolute temperature; n = 1 for the 1:1 ionic surfactant in the presence of a swamping amount of 1:1 electrolyte;[6] and R = 8.314 J mol^{-1} K^{-1}. All the physicochemical parameters of C_{12}HVal are listed in Table 1. It can be observed that CAC and γ_{CAC} values are lower than corresponding values of conventional soaps,[29,31] which suggests that C_{12}HVal is more surface active. The same is also indicated by larger pC_{20} values.[6] On the other hand, the ratio (CAC/C_{20}) of CAC and C_{20} value, which is a measure of the tendency of the surfactant to adsorb at the air−water interface relative to the formation of aggregates, is greater than those of conventional hydrocarbon monomeric surfactants. The CAC and γ_{CAC} values are also lower than those of the corresponding sodium salt of *N*-acylamino acid.[32] The cross-sectional areas were calculated from Γ_{max} values corresponding to the two breaks of the surface tension plot (Figure 2). It is important to note that C_{12}HVal has lower A_{min} values (Table 1) which are close to the surface areas of decyl and dodecyl carboxylic acids (45 Å^2)[33] at pH 13 in a 0.13 mol kg^{-1} solution. However, the surface area of sodium laurate is reported to be 69 Å^2 in aqueous solution.[31] The smaller value of cross-sectional area in the case of C_{12}HVal is indicative of formation of large aggregates with tightly packed hydrocarbon chains.

Dynamic Light Scattering Studies. To quickly measure the size of the aggregates we performed dynamic light scattering (DLS) experiments using solutions (pH 13) of C_{12}HVal in the concentration range of 0.2 to 18 mM. The size distributions of the aggregates formed are shown in Figure 3. It can be observed that the size distribution in dilute as well as in concentrated solutions is monomodal. The distribution is very narrow at concentrations just above CAC$_1$. However, the width of the distribution and the apparent *Z*-average hydrodynamic diameter (D_h) increased in going from 0.2 to 2.0 mM. This suggests that in this concentration range, two types of aggregates are in equilibrium and the smaller aggregates are converted to larger aggregates as [C_{12}HVal] is increased beyond CAC$_2$. The average diameter of the aggregates in 0.2 mM solution is about 53 nm, which is too large for a normal spherical micelle. The latter type of aggregates for C_{12}HVal is expected to have a diameter in the range 3−5 nm.[34] The average value of D_h (157 nm)

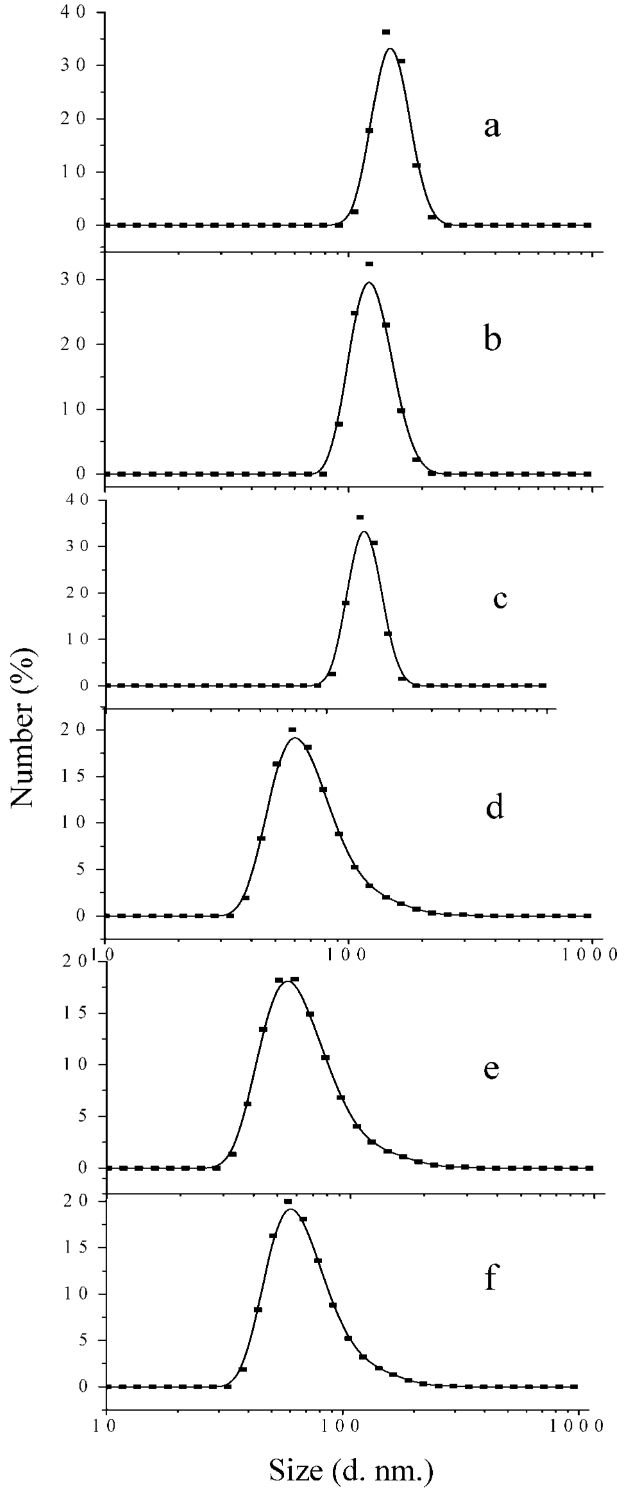

Figure 3. Size distribution of the aggregates in (a) 0.2, (b) 0.5, (c) 0.8, (d) 2.0, (e) 9.0, and (f) 18.0 mM solutions of C_{12}HVal.

reached a maximum at around 0.8 mM and then fell off to 112 nm at 2.0 mM, which remained almost unchanged thereafter. The large size of the aggregates formed in dilute as well as in concentrated solutions is indicative of the presence of either rod-like micelles or spherical and/or tubular vesicles.

Viscosity of Surfactant Solutions. The formation of rod-like or worm-like micelles is normally manifested by the increase of bulk viscosity of surfactant solution.[35–39] Therefore, we have measured the relative viscosity of aqueous solutions of C_{12}HVal at different concentrations. The variation of relative viscosity with [C_{12}HVal] is shown by the plot in Figure 4. As can be observed the viscosity increased nonlinearly up to a concentration of 15 mM and then starts to fall off at higher concentration. However, the increase of viscosity relative to that of water (pH 13) is very small even in the presence of 10 mM C_{12}HVal. Therefore, rod-like or worm-like micelles probably do not exist at all in solutions of [C_{12}HVal] < 20 mM.

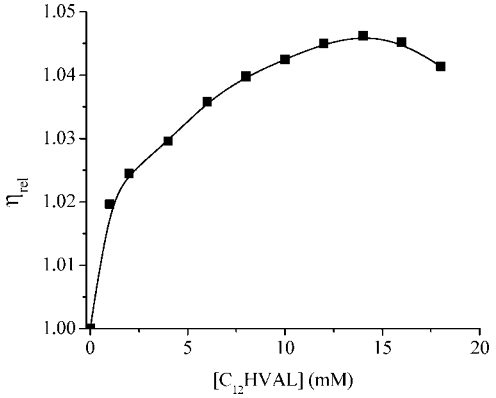

Figure 4. Plot of relative viscosity (η_{rel}) versus [C_{12}HVal].

Shape of the Aggregates. Shapes of the spontaneously formed aggregates of surfactants can be predicted with considerable certainty by using three nominal geometric parameters of the surfactant molecule: (i) the critical chain length (l_c), which is the maximum effective length the chain can assume, (ii) the volume (v) of the hydrocarbon tail, which is assumed to be fluid and incompressible, and (iii) the optimal head group area (A_{min}). Israelachvili defined a critical packing parameter or shape factor, P ($=v/l_cA_{min}$), that can be used to predict which structures an amphiphile will assemble to form.[40] The model predicts formation of spherical micelle at $P \leq {}^1/_3$, a cylindrical micelle at ${}^1/_3 \leq P \leq {}^1/_2$, a vesicle or flexible bilayer at ${}^1/_2 \leq P \leq 1$, and inverted micelles at $P > 1$. That is the parameter P is a measure of local curvature; large values of P correspond to large (or inverted) aggregates, while small values are characteristic of highly curved micellar structures. The v value for the dodecyl chain (371.9 Å^3) of C_{12}HVal was estimated from the molar volume of *n*-dodecane (368 Å^3)[41] after correction for the −OH group according to Edward's atomic increment method.[41] To obtain the value of l_c, we first optimized the geometry of the surfactant molecule using a standard MM2 force field. The linear distance (14.02 Å) between the carbon atom linked to the −NH− group and the methyl carbon at the end of the chain was taken as the critical chain length. The P values (Table 1) for both types of aggregates were calculated by using the corresponding A_{min} values obtained from surface tension studies. Both P values are greater than 0.5 suggesting spontaneous formation of bilayer aggregates. The accuracy of this estimation is proven by the experimental results described below. It is interesting to note that the P value of the bilayer assembly formed at concentrations greater than CAC_2 is higher than that of its precursor bilayer assembly. Yan et al. have shown that the P value for tubes is larger than that for vesicles.[42] They found tubes in the $0.7 \leq P \leq 1$ region and vesicles in the $0.5 \leq P \leq 0.7$ region. This suggests that in the case of C_{12}HVal, the vesicles formed in dilute solution are spontaneously converted to tubes, which is consistent with the results of surface tension and DLS studies.

Conductivity Studies. It has been reported by one of us[21b] as well as by others[43,44] that the electrical conductivity of KCl solution decreases upon addition of vesicle-forming surfactants. The vesicles entrap a part of the solvent and the salt and thereby prevent the entrapped charge carriers (K^+ and Cl^- ions) from

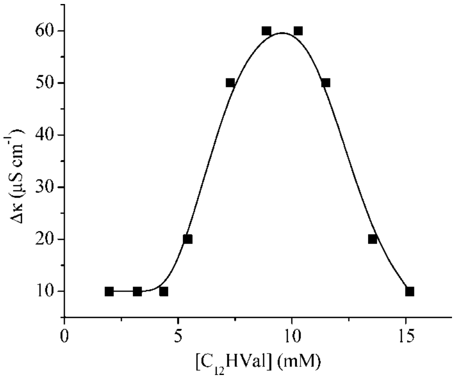

Figure 5. Characteristic conductivity change, Δ*κ*, as a function of [C$_{12}$HVal] in the presence of 5 mM KCl (0.1 M NaOH) at 30 °C.

contributing to the conductivity of the solution. Consequently, the conductivity of the vesicular solution becomes lower than the conductivity of the salt solution. To demonstrate the formation of closed vesicles/tubules by C$_{12}$HVal, we have measured conductivity of 5 mM KCl in the presence of different concentrations of the surfactant at 30 °C. It was observed that the sum of the conductivities of the solutions of 5 mM KCl and 1 mM C$_{12}$HVal (0.1 M NaOH) was greater than that of 1 mM C$_{12}$HVal (0.1 M NaOH) containing 5 mM KCl. This means that the conductivity of the KCl solution decreased in the presence of 1 mM (>CAC$_1$) C$_{12}$HVal. In contrast, no significant decrease of conductivity of the KCl solution was observed in the presence of the surfactant having a concentration less than CAC$_1$. The variation of conductivity change (Δ*κ*) with the increase of [C$_{12}$HVal] is shown in Figure 5. It can be observed that although the initial value of Δ*κ* is small, it increases with surfactant concentration and then falls off passing through a maximum. The feature of the plot in Figure 5 is very similar to the plot in Figure 4. This is a clear evidence of the formation of vesicles or tube-like structures that have an aqueous core. Since the population of vesicles/tubules increases with surfactant concentration, more K^+ and Cl^- ions become trapped inside the aqueous core and hence increase the Δ*κ* value. The decrease in Δ*κ* at high surfactant concentrations could be attributed to the transformation of closed vesicles/tubules to porous vesicles or open tubules and/or rod-like micelles.

Transmission Electron Microscopy. Transmission electron microscopy (TEM) is a particularly suitable technique for the direct visualization of the microstructure of surfactant aggregates ranging in size from about 5−10 nm to 1 *μ*m. TEM pictures of negatively stained specimens prepared from different aqueous C$_{12}$HVal solutions are shown in Figure 6. The micrograph A of the 0.3 mM solution of C$_{12}$HVal reveals spherical vesicles with diameters in the range 20−70 nm. However, micrograph B corresponding to 2 mM C$_{12}$HVal solution shows the existence of large cylindrical aggregates having a diameter in the range 20−50 nm. The micrographs are consistent with the results of surface tension and DLS measurements suggesting stepwise aggregation. Although by looking at the micrograph it may appear that these large aggregates are rod-like micelles, it can be ruled out on the basis of the fact that rod-like micelles cannot have a diameter greater than twice the length of the hydrocarbon chain length of the surfactant. That the long cylindrical aggregates are not rods is further substantiated by the observation that a concentrated solution of the amphiphile is nonviscous. Although solutions containing branching rod-like micelles are known to be fluid[45–50] in nature, the TEM images (B−E) clearly reveal the existence of tube-like structures. If the structures observed in micrographs B and E were rod-like micelles, then the solutions would be viscous as such long rods would be flexible and thus are expected to entangle with each other. Thus the larger diameter (20−50 nm) of the aggregates clearly suggests the formation of hollow tubular structures. It is interesting to observe that the tubules have branches or are connected to other tubules (micrograph C) at a relatively higher concentration (~10 mM). Micrograph D clearly shows a Y-shaped junction between tubular aggregates. The tubules are a few micrometers long and have an inner diameter of about 50−80 nm. However, the size of the aggregates as observed in the micrographs is not consistent with that obtained from DLS measurements. This is perhaps because the latter measurement, which gives an average diameter of an equivalent hard sphere, used filtered solution. Despite the tubules being connected with each other to form networks, the aqueous solutions of the amphiphiles were observed to be nonviscous. It is also interesting to observe that at a much higher concentration (~18 mM) of C$_{12}$HVal the junctions are broken and tubules are separated into individual tubules (see micrograph E) which appear to be open at both ends. It appears that the contour lengths of the tubules do not change significantly with the rise of concentration. The hollowness of the structures is clearly visible from the broken surface of the tubules.

Although the staining method of obtaining the TEM image is often criticized, the above-mentioned microstructures of the self-assemblies of C$_{12}$HVal were not observed with C$_{12}$Val (results not included), which is structurally similar but lacks the −OH group present in the hydrocarbon chain of C$_{12}$HVal. This means that the microstructures shown in the TEM images are real, not artifacts. The effect of high salt concentration on the formation of worm-like micelles was also eliminated by the observations that the viscosity of the surfactant solution (10 mM) did not change significantly in the presence of 150 mM NaCl (much higher than 1.5% sodium phosphotungstate).

On the basis of theoretical calculations, many authors have proposed different models for the formation of tubules. These have been critically discussed in an article by Selinger and coworkers.[51] Chen[52] has proposed a kinetic pathway for tubule formation without taking chirality into account. According to this mechanism, the amphiphiles initially self-assemble to form spherical vesicles at higher temperature. The redistribution of molecules between the inner and outer layer then breaks the bilayer symmetry giving the membrane a spontaneous curvature. When the system is cooled the vesicle membrane distorts to form a cylindrical tubule having a radius of half of the vesicle radius. This model has also been criticized by others including Selinger.[50] According to these authors tubules are formed by the twisting of flat bilayers through the formation of helical ribbons as an intermediate structure. This model provides an explanation for the helical markings that are often seen in the electron micrographs of tubules.[53–56] In the case of C$_{12}$HVal, however, no such marking on the tubes can be seen. An alternative pathway for the formation of tubules could be rolling of the flat bilayer like a cigarette paper. But this does not explain the formation of Y-type junctions. In fact, none of the proposed theoretical models have attempted to explain the branching of tubular structures.

It is important to note that in the case of C$_{12}$HVal the concentration-dependent stepwise aggregation is indicated by the surface tension as well as fluorescence studies. Conductivity measurements also indicated transformation of closed vesicles to branching tubules to open tubules with the increase of [C$_{12}$HVal]. This is further supported by the concentration dependence of aggregate size distribution. The TEM pictures

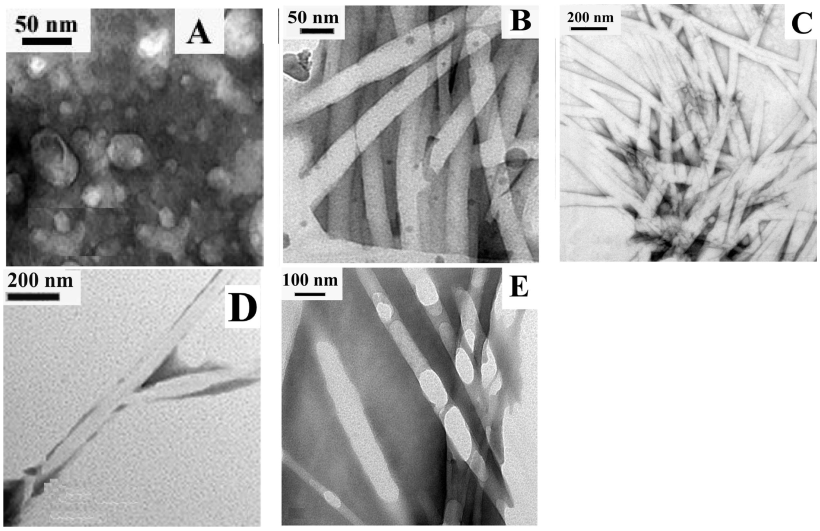

Figure 6. Negatively stained (with aqueous 1.5% phosphotungstate) TEM micrographs of (A) 0.3, (B) 2.0, (C, D) 10, and (E) 18 C_{12}HVal in water, pH 13 at 30 °C.

are consistent with the results of DLS studies. It is clear that C_{12}HVal produce spherical vesicles in dilute solution, which upon increase of surfactant concentration transform into branching tubules through fusion. However, no bilayer structure, such as vesicles or tubules, was observed with the structurally similar amphiphile C_{12}Val in the concentration range employed. Therefore, it is clear that the hydrogen-bonding interaction between −OH and −NH groups of adjacent amphiphiles might be responsible for the formation of bilayer structures. We believe that small tubules are first formed at amphiphile concentration just above the second CAC, which then grow into large tubes with Y-junctions when the concentration is increased further. Micellar branching in solutions of nonionic,[57] ionic,[45–50] and mixed surfactant systems[58–60] has been reported. In fact, Porte et al.[61] first suggested the occurrence of micellar branching. As discussed elsewhere the entropic factor is responsible for micellar defects, such as "end caps" or "Y-junctions".[40] Perhaps the arguments based on entropic factor proposed for the structural defects in rod-like micelles can be applied for the formation of branching tubules by C_{12}HVal. However, it is not clear to us at this moment why the network structure is broken at higher concentrations. Further work is currently underway in this laboratory to understand the mechanism of formation of branching tubules by structurally similar molecules.

Conclusions

In summary an *N*-alkylamino acid-derived amphiphile C_{12}HVal was synthesized and its surface properties and aggregation behavior were studied in aqueous solutions at pH ∼13. The amphiphile is more surface active than the corresponding fatty acid salt. Both surface tension and fluorescence measurements suggested that the amphiphile exhibits stepwise aggregate formation characterized by two CAC values. Below CAC_2 only spherical vesicles are formed as indicated by the electron micrographs. However, at concentrations above CAC_2, the tubular structures exist in solution. The tube-like structures have a packing parameter of $0.7 \leq P \leq 1$ whereas vesicles have a packing parameter in the $0.5 \leq P \leq 0.7$ region. The TEM pictures revealed the existence of tubules with Y-type junctions at higher concentrations of C_{12}HVal amphiphile. The branching tubules of the C_{12}HVal amphiphile are converted to straight long tubules at higher surfactant concentrations above CAC_2. Like solutions containing branched worm-like micelles the aqueous solutions of branched tubules are nonviscous. To our knowledge, this is the first report on the formation of branching tubules by an ionic amphiphile. However, the structurally similar amphiphile C_{12}Val failed to form any bilayer structure in the concentration range employed. Thus, it may be speculated that the hydrogen-bonding interaction between −OH and −NH groups of adjacent amphiphiles is responsible for the formation of bilayer structures of C_{12}HVal. A detailed investigation with other structurally similar amino acid derivatives is being carried out in this laboratory to demonstrate the role of hydrogen-bonding interaction.

Experimental Section

Materials. The amphiphile *N*-(2-hydroxy-*n*-dodecyl)-L-valine (C_{12}HVal) was prepared according to the procedure described elsewhere[16] and was purified by recrystallization from ethanol or ethanol−water mixture. The chemical structure of the amphiphile was identified and checked for purity by the usual methods (IR, ^{1}H NMR, TLC). 1,2-Epoxydodecane (Aldrich) and L-valine (SRL, Mumbai) were used without further purification. The fluorescent probe *N*-phenyl-1-naphthylamine, NPN (Aldrich), was recrystallized several times from ethanol−water mixture. All solvents used were obtained locally and were distilled and dried whenever required. Analytical grade sodium hydroxide and hydrochloric acid were procured locally and were used directly from the bottle.

Methods. The ^{1}H and ^{13}C NMR spectra were recorded on a Bruker 400 MHz instrument. Surface tension measurements were carried out with a surface tensiometer (model 3S, GBX, France), using the Du Nuöy ring detachment method. All the solutions containing different concentrations of C_{12}HVal were prepared at pH 13 by using double distilled water and 1 N sodium hydroxide and were stored in closed glass bottles. Conductivity was measured with a Thermo Orion conductivity meter (model 150 A+) by use of a cell having a cell constant equal to 0.467 cm^{-1}. Ph measurements were done with a Thermo Orion (model 710 A+) pH meter, using a combined glass electrode. Relative viscosity of solutions was measured by use of a glass Ubbelohde viscometer (ASTM-D-446) with a flow time of 180 s for pure water. The density measurement was performed by use of a portable digital density meter (Densito 30 PX, Mettler-Toledo, GmbH). All measurements were carried out at room temperature (∼30 °C) unless otherwise mentioned.

Steady-state fluorescence spectra of NPN were recorded on a Perkin-Elmer LS-55 fitted with a thermostating cell holder and a polarizer in the L-format configuration. A fixed excitation band-pass of 2.5 nm and emission band-pass in the range 2.5−5.0 nm was used for the measurement of emission spectra. A saturated solution of NPN in water (pH 13) was used to prepare surfactant solutions of varying concentration. The samples containing NPN were excited at 340 nm. Uncorrected emission spectra were recorded in the range 360−550 nm.

The dynamic light scattering (DLS) measurements were performed with a Zetasizer Nano ZS (Malvern Instrument Laboratory, Malvern, U.K.) optical system equipped with an He−Ne laser operated at 4 mW at $\lambda_o = 632.8$ nm, and a digital correlator. The solution was filtered directly into the scattering cell through a Millipore Millex syringe filter (Triton free, 0.45 μm). Before measurement, the scattering cell was rinsed several times with the filtered solution. The DLS measurements started 10 min after the sample solutions were placed in the DLS optical system to allow the sample to equilibrate at 30 °C. The scattering intensity was measured at a 173° angle to the incident beam. The data acquisition was carried out for 2 min and each experiment was repeated at least two times. Apparent diffusion coefficients (D_{app}) were calculated by cumulant analysis of an autocorrelation function of scattered light intensity fluctuations. Effective hydrodynamic radii (R_h) were calculated from diffusion coefficients, using the Stokes−Einstein equation:

$$D_{app} = k_B T / 6\pi\eta R_h \tag{3}$$

where k_B is the Boltzmann constant, T is the absolute temperature, and η is the viscosity of the solvent.

The samples for TEM were prepared according to the usual procedure. A 5 μL sample of the surfactant solution (pH 13) was placed on the 400 mesh carbon-coated copper grid and allowed to adsorb for a minute. The excess liquid was then wicked off with a filter paper, air-dried, and negatively stained with freshly prepared 1.5% aqueous sodium phosphotungstate (pH 13). The specimens were dried overnight in desiccators before measurement with an electron microscope (JEOL-JEM 2100, Japan) operating at 200 kV.

Acknowledgment. The authors gratefully acknowledge CSIR, New Delhi for financial support (Grant No. 01(2008)/05/EMR-II) of this work. A.G. thanks CSIR (09/081(0542)/2005-EMR-I) for a research fellowship. The authors are thankful to Dr. A. Dasgupta, Department of Biochemistry, Calcutta University, Kolkata for assistance with the DLS measurements.

References and Notes

(1) Lehn, J. M. *Science* **1993**, *260*, 1762–1763.

(2) Whitesides, G. M.; Mathias, J. P.; Seto, C. T. *Science* **1991**, *254*, 1312–1319.

(3) Spector, M. S.; Price, R. R.; Schnur, J. M. *Adv. Mater.* **1999**, *11*, 337–340.

(4) Ai, S.; Lu, G.; He, Q.; Li, J. *J. Am. Chem. Soc.* **2003**, *125*, 11140–11141.

(5) Matsui, H.; Douberly, G. E. J. *Langmuir* **2001**, *17*, 7918–7922.

(6) Rosen, M. J. *Surfactants and Interfacial Phenomena*, 4th ed.; Wiley-Interscience; New York, 2004.

(7) (a) Laughlin, R. G. *The aqueous phase behavior of surfactants*; Academic Press: London, UK, 1994. (b) Evans, D. F.; Myers, D. *Surfaces, Interfaces and Colloids: Principles and Applications*; VCH; New York, 1991.

(8) Schnur, J. M. *Science* **1993**, *262*, 1669–1676.

(9) Fuhrhop, J. H.; Helfrich, W. *Chem. Rev.* **1993**, *93*, 1565–1582.

(10) Emmanouil, V.; Ghoul, M. El; Andre-Barres, C.; Guidetti, B.; Rico-Lattes, I.; Lattes, A. *Langmuir* **1998**, *19*, 5389–5395.

(11) Köning, J.; Boettcher, C.; Winkler, H.; Zeitler, E.; Talmon, Y.; Fuhrhop, J. H. *J. Am. Chem. Soc.* **1997**, *115*, 693–900.

(12) Sylvain, V.; Santoso, S.; Gong, H.; Watson, N.; Zhang, S. *Proc. Natl. Acad. Sci. U.S.A.* **2002**, *99*, 5355–5360.

(13) Bong, D. T.; Clark, T. D.; Granja, J. R.; Ghadiri, M. R. *Angew. Chem., Int. Ed.* **2001**, *40*, 988–1011.

(14) Fernandez-Lopez, S.; Kim, H. S.; Choi, E. C.; Delgado, M.; Granja, J. R.; Khasanov, A.; Kraehenbuehl, K.; Long, G.; Weinberger, D. A.; Wilcoxen, K. M.; Gghadiri, M. R. *Nature (London)* **2001**, *41*, 452–455.

(15) (a) Yan, Y.; Huang, J.; Li, Z.; Han, F.; Ma, J. *Langmuir* **2003**, *19*, 972–974. (b) Han, F.; He, X.; Huang, J.; Li, Z.; Wang, Y.; Fu, H. *J. Phys. Chem. B* **2004**, *108*, 5256–5262. (c) Lu, T.; Han, F.; Li, Z.; Huang, J.; Fu, H. *Langmuir* **2006**, *22*, 2045–2049.

(16) Hidaka, H.; Murata, M.; Onai, T. *Chem. Commun.* **1984**, *562*, 564.

(17) Imae, T.; Takahasshi, Y.; Muramatsu, H. *J. Am. Chem. Soc.* **1992**, *114*, 3414–3419.

(18) Bhattacharya, S.; Haldar, J. *Langmuir* **2004**, *20*, 7940–7947.

(19) Won, Y.-Y.; Brannan, A. K.; Davis, H. T.; Bates, F. S. *J. Phys. Chem. B* **2002**, *106*, 3354–3364.

(20) Hassan, P. A.; Raghavan, S. R.; Kaler, E. W. *Langmuir* **2002**, *18*, 2543–2548.

(21) (a) Roy, S.; Dey, J. *Bull. Chem. Soc. Jpn.* **2006**, *79*, 59–66. (b) Roy, S.; Dey, J. *Langmuir* **2005**, *21*, 10362–10369.

(22) Saitoh, T.; Taguchi, K.; Hiraide, M. *Anal. Chim. Acta* **2002**, *454*, 203–208.

(23) Félix, M.; Goñi, A. A. *Biochim. Biophys. Acta* **2000**, *1508*, 51–68.

(24) Saitoh, T.; Matsushima, S.; Hiraide, M. *Colloids Surf., A* **2007**, *299*, 88–92.

(25) Nemkovich, N. A.; Baumann, W.; Kruchenok, Y. V.; Reis, H.; Rubinov, A. N. *J. Fluoresc.* **1997**, *7*, 363–370.

(26) Nayak, R. R.; Roy, S.; Dey, J. *Colloid Polym. Sci.* **2006**, *285*, 219–224.

(27) Roy, S.; Nayak, R. R.; Dey, J. *Colloids Surf., A* **2006**, *290*, 62–69.

(28) Khatua, D.; Dey, J. *J. Phys. Chem. B* **2007**, *111*, 124–130.

(29) Pegiadou, S.; Perez, L.; Infante, M. R. *J. Surfactants Deterg.* **2000**, *3*, 517–524.

(30) Varka, E. M.; Coutouli-Argyropoulou, E.; Infante, M. R.; Pegiadou, S. *J. Surfactants Deterg.* **2004**, *7*, 409–414.

(31) Ono, D.; Masuyama, A.; Nakatsuji, Y.; Okahara, M.; Yamamara, S.; Takeda, T. *J. Am. Oil Chem. Soc.* **1993**, *70*, 29–36.

(32) George, A.; Jain, N.; Desai, A.; Bahadur, P. *Tenside Surfactants Deterg.* **1998**, *35*, 368–374.

(33) Huang, J.-B.; Mao, M.; Zhu, B.-Y. *Colloids Surf., A* **1999**, *155*, 339–348.

(34) Singh, M.; Trivedi, M. K.; bellare, J. *J. Mater. Sci.* **1999**, *34*, 5315–5323.

(35) Kaler, E. W.; Herrington, K. L.; Iampietro, D. J.; Coldren, B.; Jung, H. T.; Zasadzinski, J. A. In *Mixed Surfactant Systems*, 2nd ed.; Abe, M., Scamehorn, J., Eds.; Marceel Dekker: New York, 2005.

(36) Angeleseu, D.; Khan, A.; Caldaram, H. *Langmuir* **2003**, *19*, 9155–9161.

(37) Hassan, P. A.; Yakhmi, J. V. *Langmuir* **2000**, *16*, 7187–7191.

(38) Soltero, J. F.A.; Puig, J. E. *Langmuir* **1996**, *12*, 2654–2662.

(39) Pal, O. R.; Gaikar, V. G.; Joshi, J. V.; Goyal, P. S.; Aswal, V. K. *Langmuir* **2002**, *18*, 6764–6768.

(40) Israelachvili, J. N. *Intermolecular and Surface Forces*, 2nd ed.; Academic Press: New York, 1991.

(41) Edward, E. T. *J. Chem. Educ.* **1970**, *47*, 261–270.

(42) Yan, Y.; Xiong, W.; Li, X.; Lu, T.; Huang, J.; Li, Z.; Fu, H. *J. Phys. Chem. B* **2007**, *111*, 2225–2230.

(43) Horbaschek, K.; Hoffmann, H.; Thunig, C. *J. Colloid Interface Sci.* **1998**, *206*, 439–456.

(44) Shankar, B. V.; Patanaik, A. *Langmuir* **2007**, *23*, 3523–3529.

(45) Gonzalez, Y. I.; Kaler, E. W. *Curr. Opin. Colloid Interface Sci.* **2005**, *10*, 256–260.

(46) Shashkina, J. A.; Philoppova, O. E.; Zaroslov, Y. D.; Khokhlov, A. R.; Pryikhina, T. A.; Blagodatskikh, I. V. *Langmuir* **2005**, *21*, 1524–1530.

(47) Flood, C.; Dreiss, C. A.; Croce, V.; Cosgrove, T.; Karlsson, G. *Langmuir* **2005**, *21*, 7646–7652.

(48) Schubert, B. A.; Kaler, E. W.; Wagner, N. J. *Langmuir* **2003**, *19*, 4079–4089.

(49) Raghavan, S. R.; Edlund, H.; Kaler, E. W. *Langmuir* **2002**, *18*, 1056–1064.

(50) Bernheim-Groswasser, A.; Zana, R.; Talmon, Y. *J. Phys. Chem. B* **2000**, *104*, 4005–4009.

(51) Selinger, J. V.; Spector, M. S.; Schnur, J. M. *J. Phys. Chem. B* **2001**, *105*, 7157–7169.

(52) Chen, C. M. *Phys. Rev. E* **1999**, *59*, 6192–6195.

(53) Blanzat, M.; Massip, S.; Spéziale, V.; Perez, E.; Rico-Lattes, L. *Langmuir* **2001**, *17*, 3512–3514.

(54) Fuhrop, J. H.; Blumtritt, P.; Lehmann, C.; Luger, P. *J. Am. Chem. Soc.* **1991**, *113*, 7437–7439.

(55) Spector, M. S.; Selinger, J. V.; Singh, A.; Rodriguez, J. M.; Price, R. R.; Schnur, J. M. *Langmuir* **1998**, *14*, 3493–3500.

(56) Spector, M. S.; Selinger, J. V.; Schnur, J. M. *J. Am. Chem. Soc.* **1997**, *119*, 8533–8539.

(57) Bernheim-Groswasser, A.; Watchtel, E.; Talmon, Y. *Langmuir* **2000**, *16*, 4131–4140.

(58) Bernheim-Groswasser, A.; Zana, R.; Talmon, Y. *J. Phys. Chem. B* **2000**, *104*, 12192–12201.

(59) Koehler, R. D.; Raghavan, S. R.; Kaler, E. W. *J. Phys. Chem. B* **2000**, *104*, 11035–11044.

(60) Kwon, S. Y.; Kim, M. W. *Phys. Rev. Lett.* **2002**, *89*, 258302–258304.

(61) Porte, G.; Gomati, R.; Haitami, O. E.; Appell, J.; Marignan, J. *J. Phys. Chem.* **1986**, *90*, 5746–5751.

JP712111D